SHARPIN is a novel gene of colorectal cancer that promotes tumor growth potentially via inhibition of p53 expression

YUSUKE NAKANO[1,2], TAKAAKI MASUDA[1,3], TAKEHARU SAKAMOTO[4], NORITAKA TANAKA[4], TARO TOBO[5], MASAHIRO HASHIMOTO[1,2], TAKANARI TATSUMI[1], HIDEYUKI SAITO[1], JUNICHI TAKAHASHI[1], KENSUKE KOIKE[1], TADASHI ABE[1], YUKI ANDO[1], YUKI OZATO[1,2], KIYOTAKA HOSODA[1], KOSUKE HIROSE[1], SATOSHI HIGUCHI[1,2], TOMOHIKO IKEHARA[1], YUICHI HISAMATSU[1], TAKEO TOSHIMA[1], YUSUKE YONEMURA[1], TAKAYUKI OGINO[2], MAMORU UEMURA[2], HIDETOSHI EGUCHI[2], YUICHIRO DOKI[2] and KOSHI MIMORI[1]

[1]Department of Surgery, Kyushu University Beppu Hospital, Oita 874-0838, Japan; [2]Department of Gastroenterological Surgery, Graduate School of Medicine, Osaka University, Osaka 565-0871, Japan; [3]Department of Breast and Endocrine Surgery, Kochi Medical School, Kochi University, Nankoku 783-8505, Japan; [4]Department of Cancer Biology, Institute of Biomedical Science, Kansai Medical University, Osaka 573-1010, Japan; [5]Department of Clinical Laboratory Medicine, Kyushu University Beppu Hospital, Oita 874-0838, Japan

Received February 13, 2024; Accepted September 26, 2024

DOI: 10.3892/ijo.2024.5701

Abstract. Colorectal cancer (CRC) is widely prevalent and represents a significant contributor to global cancer-related mortality. There remains a pressing demand for advancements in CRC treatment modalities. The E3 ubiquitin ligase is a critical enzyme involved in modulating protein expression levels via posttranslational ubiquitin-mediated proteolysis, and it is reportedly involved in the progression of various cancers, making it a target of recent interest in anticancer therapy. In the present study, using comprehensive expression analysis involving spatial transcriptomic analysis with single-cell RNA sequencing in clinical CRC datasets, the ubiquitin-associated protein Shank-associated RH domain interactor (*SHARPIN*) was identified, located on amplified chromosome 8q, which could promote CRC progression. *SHARPIN* was found to be upregulated in tumor cells, with elevated expression observed in tumor tissues. This heightened expression of *SHARPIN* was positively associated with lymphatic invasion and served as an independent predictor of a poor prognosis in patients with CRC. *In vitro* and *in vivo* analyses using SHARPIN-overexpressing or -knockout CRC cells revealed that SHARPIN overexpression upregulated MDM2, resulting in the downregulation of p53, while SHARPIN silencing or knockout downregulated MDM2, leading to p53 upregulation, which affects cell cycle progression, tumor cell apoptosis and tumor growth in CRC. Furthermore, *SHARPIN* was found to be overexpressed in several cancer types, exerting significant effects on survival outcomes. In conclusion, SHARPIN represents a newly identified novel gene with the potential to promote tumor growth following apoptosis inhibition and cell cycle progression in part by inhibiting p53 expression via MDM2 upregulation; therefore, SHARPIN represents a potential therapeutic target for CRC.

Correspondence to: Professor Koshi Mimori, Department of Surgery, Kyushu University Beppu Hospital, 4546 Tsurumibaru, Oita 874-0838, Japan
E-mail: mimori.koshi.791@m.kyushu-u.ac.jp

Key words: colorectal cancer, shank-associated RH domain interactor, novel gene, p53, ubiquitin-proteasome system

Introduction

The ubiquitin (Ub)-proteasome system (UPS) is a complex and essential cellular machinery responsible for regulating protein expression levels by degrading intracellular proteins in eukaryotic cells (1). This system plays a pivotal role in maintaining cellular homeostasis by controlling the concentration of specific proteins, thus ensuring the timely removal of misfolded, damaged, or no longer needed proteins (2). The UPS plays crucial roles in multiple essential cellular processes, such as advancing the cell cycle, transmitting signals, repairing DNA, and modulating immune response (3). In the UPS, three key enzymes operate in enzyme cascades to transfer ubiquitin to the substrate: the ubiquitin-activating enzyme (E1), ubiquitin-conjugating enzyme (E2), and ubiquitin-protein ligase (E3) (4). The UPS process follows these steps: initially, E1 activates Ub and transfers it to E2 in an adenosine triphosphate-dependent manner. Then, E3 facilitates the final step by interacting with E2 to transfer Ub and identify a specific substrate (5). E3 is crucial in this enzyme cascade as its interaction with the substrate is highly specific, and the ubiquitination of the substrate primarily depends on E3 (6).

The UPS, especially E3, significantly contributes to cancer development. Aberrant E3 activity has been widely reported in various cancers. For instance, RNF6 has been shown to promote the progression of colorectal cancer (CRC) by

facilitating the ubiquitination of TLE3 (7,8). Moreover, E3 has the capacity to control downstream substrates, encompassing numerous oncogenes and tumor suppressors. For instance, it has been reported that the E3 ligase RING1 mediates the degradation of TP53 (9). Therefore, an increasing endeavor exists to find safe and bioavailable compounds that specifically target E3 ligases for cancer treatment. Several such compounds targeting key E3 ligases, including MDM2, SKP2, BTRC, TRAF6 and PRC1 (10-16), have already been developed, with some demonstrating antitumor efficacy in CRC. Given these advancements, it is becoming increasingly imperative to discover additional E3 ligase-related genes as potential novel targets.

LUBAC (Linear Ubiquitin Chain Assembly Complex) is an important E3 ubiquitin ligase complex consisting of HOIL-1L (heme-oxidized IRP2 ubiquitin ligase 1), HOIP (HOIL-1 interacting protein), and SHARPIN (SHANK-associated RH domain interactor), which plays a critical role in various cellular processes, including immune responses, inflammation and cell survival (17). SHARPIN is crucial for LUBAC's structural integrity and stability, interacting with HOIP and HOIL-1L to ensure proper assembly and function (18,19). Additionally, SHARPIN regulates various signaling pathways by modulating LUBAC's activity. Specifically, SHARPIN adjusts the enzymatic activity of LUBAC, which in turn optimizes immune responses, inflammation and cell survival pathways (18,20).

Chromosome amplification is recognized as a significant driver of cancer advancement (21). The current findings indicated that the amplification of various chromosomes, notably chromosome 8 (Ch.8), is a key and prevalent occurrence in CRC development (22,23). Previously, a screening system utilizing bioinformatics and publicly available datasets was developed by the authors to identify candidate genes that promote tumor growth within amplified chromosomes in solid tumors (24-26). This approach allows for thorough exploration of candidate therapeutic targets that are overexpressed as a result of DNA copy number amplification in CRC cells.

In the present study, SHARPIN was identified on Ch.8q, which could promote tumor growth and serves as a potential therapeutic target in CRC using our screening system, including single-cell RNA sequencing (scRNA-seq) and spatial transcriptomic expression analyses, combined with *in vitro* and *in vivo* analyses.

Materials and methods

Public datasets. The CRC mRNA expression data from The Cancer Genome Atlas (TCGA) was downloaded from UCSC Xena (http://xena.ucsc.edu/). The gene-level transcription estimates were obtained as log2(x+1) transformed RSEM normalized counts. Additionally, *SHARPIN* mRNA expression and DNA copy number data for CRC cell lines were acquired from the Cancer Cell Line Encyclopedia (https://www.broadinstitute.org/ccle/home). Furthermore, mutation annotation data from 2561 patients with CRC were obtained from the Catalogue of Somatic Mutations in Cancer (COSMIC) database (https://cancer.sanger.ac.uk/cosmic). Data pertaining to E3 ubiquitin ligases were also obtained from the Database of Human E3 Ubiquitin Ligases (https://esbl.nhlbi.nih.gov/Databases/KSBP2/Targets/Lists/E3-ligases/) (27). The single-cell RNA sequencing dataset (scRNA-seq) was attained from GSE178341 and the spatial transcriptomic dataset (ST-seq) was obtained from the spatial transcriptomic research website (http://www.cancerdiversity.asia/scCRLM/). The ST-seq data from a patient identified as ST-P1, who did not undergo neoadjuvant chemotherapy treatment, were utilized for analysis.

Patients with CRC and clinical sample collection. Primary CRC samples were obtained from our CRC cohort comprising 111 patients (clinicopathological characteristics including sex and age distribution are listed in Table I) who underwent surgery at Kyusyu University Beppu Hospital and affiliated hospitals from January 1993 to December 2002. The inclusion criteria were as follows: i) Patients who were confirmed to have CRC by post-operative pathological analysis; ii) patients who had not received any pre-operative radiotherapy, chemotherapy or other related treatments; and iii) the patient medical records were complete. The exclusion criterion was a history of malignant tumor treatment in other parts of the body. All patients were treated in accordance with the Japanese Society of Cancer of the Colon and Rectum Guidelines for the Treatment of CRC (28). The present study was approved by the Kyushu University Institutional Review Board (approval no. 22244-00; Oita, Japan), and informed consent was obtained in the form of opt-out on the following website: https://www.beppu.kyushu-u.ac.jp/geka/information/clinical_disclosure/. Those who opted out were excluded. Tumor tissues that were surgically removed, along with corresponding tumour adjacent normal tissues, as well as formalin-fixed paraffin-embedded sections, were obtained from patients with CRC as previously described (24).

Selection of candidate genes. The TCGA dataset was used to identify candidate genes from among 665 genes located on Ch.8q, adhering to the following three criteria: i) Overexpression in tumor tissues compared with normal tissues ($P<0.01$); ii) positive correlation between DNA copy number and mRNA expression levels (correlation coefficient cut-off=0.7); and iii) high mRNA expression significantly associated with poor prognosis ($P<0.05$). Genes identified through this approach were classified as candidate genes implicated in CRC triggered by Ch.8q amplification (Fig. S1A).

Pan-cancer analysis. Raw count and quantile-normalized mRNA data were collected from the TCGA dataset for all cancer types. Cancer types with fewer than 10 normal tissues available for comparison were excluded from our analysis. mRNA expression levels in the listed cancers were contrasted with those in the corresponding non-cancerous tissues.

Cell lines and cell culture. The human CRC cell lines were obtained from the following sources: RKO (cat. no. CRL-2577), HT29 (cat. no. HTB-38), and LS174T (cat. no. CL-188) from the ATCC; LoVo (cat. no. JCRB9083), Colo201 (cat. no. JCRB0226), DLD-1 (cat. no. JCRB9094), WiDr (cat. no. IFO50043), CaR1 (cat. no. JCRB0207), and Colo320DM (cat. no. JCRB0225) from the JCRB Cell Bank; HCT116 (cat. no. RBRC-RCB2979) and Colo205 (cat. no. RBRC-RCB2127)

Table I. Univariate and multivariate analyses of clinicopathological factors associated with overall survival in our patients with colorectal cancer.

Variable	HR	Univariate (95% CI)	P-value	HR	Multivariate (95% CI)	P-value
Age, years (≥65 vs. <65)	1.73	0.83-3.59	0.14			
Sex (male vs. female)	1.11	0.52-2.35	0.79			
Tumor size (cm) (≥3 vs. <3)	8.34	1.13-61.30	<0.05			
T stage (3/4 vs. 1/2)	6.82	0.46-4.18	<0.01	5.70	0.62-52.60	0.13
Lymphatic invasion (+ vs. -)	4.57	2.07-10.10	<0.01			
Vascular invasion (+ vs. -)	4.80	2.11-10.93	<0.01			
Lymph node metastasis (+ vs. -)	6.82	2.78-16.80	<0.01	3.21	1.28-8.36	<0.05
Distant metastasis (+ vs. -)	9.65	2.69-34.60	<0.01	3.87	1.02-14.7	<0.05
SHARPIN expression (+ vs. -)	4.99	2.03-12.30	<0.01	3.29	1.26-8.60	<0.01

CI, confidence interval; HR, hazard ratio.

from the RIKEN Cell Bank; and SW480 (cat. no. 87092801) and SW620 (cat. no. 87051203) from the ECACC. The cell lines were cultured under the following conditions: RKO, WiDr, CaR1 and LS174T were cultured in Eagle's Minimum Essential Medium (FUJIFILM Wako Pure Chemical Corporation) with non-essential amino acids (NEAA) and 10% fetal bovine serum (FBS); HCT116 and Colo320DM were cultured in Dulbecco's Modified Eagle Medium (FUJIFILM Wako Pure Chemical Corporation) with 10% FBS; LoVo was cultured in Ham's F12 medium (Gibco; Thermo Fisher Scientific, Inc.) with 20% FBS; Colo201, DLD-1, Colo205, SW480 and SW620 were cultured in RPMI-1640 medium (FUJIFILM Wako Pure Chemical Corporation) with 10% FBS; and HT29 was cultured in McCoy's 5A medium (Gibco; Thermo Fisher Scientific, Inc.) with 10% FBS. All cell lines were maintained in a humidified atmosphere containing 5% CO_2 at 37˚C.

RNA extraction and reverse-transcription quantitative polymerase chain reaction (RT-qPCR). Total RNA was extracted from cell lines and tissues utilizing ISOGEN-II (Nippon Gene Co., Ltd.). Subsequently, 1 μg of RNA underwent reverse transcription to generate cDNA using RevertAid RT Reverse Transcription Kit (cat. no. K1691; Thermo Fisher Scientific, Inc.), following the manufacturer's guidelines (Thermo Fisher Scientific, Inc.). Lightcycler 480 Instrument II (Roche Diagnostics) was used to measure the qPCR, which were carried out using LightCycler FastStart DNA Master SYBR Green I (Roche Diagnostics) in triplicate as previously described (29). The amplification protocol comprised 40 cycles, involving denaturation at 95˚C for 10 sec, annealing at 60˚C for 10 sec, and elongation at 72˚C for 20 sec. Post-amplification, the products underwent a temperature gradient from 68-95˚C at a rate of 0.2˚C/sec, with continuous fluorescence monitoring to generate a melting curve of the products. Gene expression was quantified using the following oligonucleotide primers: *SHARPIN* sense, 5'-CTCAGCCTGCACTTCCTCAA-3' and antisense, 5'-GGAAGATCTGCCTCAGGTGG-3'; and *18S* sense, 5'-AGTCCCTGCCCTTTGTACACA-3' and antisense, 5'-CGATCCGAGGGCCTCACTA-3'. The relative gene expression level was calculated using the Standard Curve Method (30,31). Gene expression levels were normalized to the expression of *18S*, serving as an internal control within each sample.

Immunohistochemical analysis. Immunohistochemical examination of CRC tissue specimens and tissue samples from mouse xenograft tumors was conducted using 3-μm thick sections, according to established protocols (32). Hematoxylin was employed for counterstaining all sections. Primary antibodies utilized included anti-SHARPIN (1:200; cat. no. 14626-1-AP; Proteintech Group, Inc.) and anti-p53 (1:100; cat. no. ab1101; Abcam). Tumor histology underwent independent assessment by two researchers, one of whom was an experienced pathologist (Taro Tobo).

Small interfering RNA-mediated knockdown. SHARPIN-specific small interfering RNAs (siRNAs) (#s37848 and #s37849) as well as a negative control siRNA (*Silencer*™ Negative Control No. 1 siRNA cat. no. AM4611) were procured from Thermo Fisher Scientific, Inc. at a concentration of 10 μM. Utilizing Lipofectamine RNAiMAX (Thermo Fisher Scientific, Inc.), the CRC cells underwent transfection with the siRNA oligonucleotides according to the manufacturer's protocol. Briefly, 250 μl of Opti-MEM™ I Reduced Serum Medium (cat. no. 31985062; Gibco; Thermo Fisher Scientific) was added to each of two DNase/RNase-Free Eppendorf (EP) tubes. One tube had 17 μl of RNAiMAX and the other had 6 μl of RNA primers. The contents of the two tubes were mixed and then left to stand for 5 min at room temperature. The cells were washed with PBS, and antibiotic-free serum medium was added to each well, followed by the transfection mixture. The cells were cultured in a CO_2 incubator at 37˚C, and the interval between transfection and subsequent experiments was ~48 h.

Generation of SHARPIN-knockout CRC cells. The lentivirus construct LentiCRISPRv2 (33,34) was obtained from Addgene, Inc., and oligo DNA of the targeted sequences was subcloned into the LentiCRISPRv2 plasmid, according

to the manufacturer's protocol. The sequences of the single guide RNAs (sgRNAs) were as follows: non-target sgRNA (NT), 5'-GCGAGGTATTCGGCTCCGCG-3', and SHARPIN sgRNA, 5'-CACCGTGCCTCTTACGGGGTTCGGC-3'. The oligo sequences were designed using the CRISPRdirect (https://crispr.dbcls.jp/; National Institute of Genetics), a web-based tool for designing guide RNAs with reduced off-target effects. The targeted region within the SHARPIN gene was exon 6, specifically chr8:144099328-144099350, which encodes a Zn-finger domain in the Ran binding protein. For the lentiviral transfection, a third-generation system was used. Lentiviral particles for infecting RKO and LoVo cells were generated by transiently co-transfecting 293FT cells with 1.25 μg of the plasmid containing the oligo DNA of the targeted sequences subcloned into the LentiCRISPRv2 plasmid and 1.8 μg of ViraPower Lentiviral Packaging Mix (Thermo Fisher Scientific, Inc.) using Lipofectamine 3000 reagent (Thermo Fisher Scientific, Inc.), following the manufacturer's protocol. After a 48-h incubation at 37˚C, a total of 2 ml viral supernatant was collected, and 1 ml was added to each of the RKO and LoVo cells. The cells were transduced at a MOI of 10 with lentiviral particles for 24 h, after which the medium was replaced. The cells were then subjected to selection using 2 μg/ml puromycin for 3 days, with 1 μg/ml puromycin used for maintenance. Subsequent experiments were then started. Non-cloned cells were utilized to maintain a heterogeneous cell population. The validation of SHARPIN knockout clones was conducted through western blot analysis and Sanger sequencing.

Generation of CRC cells with stable overexpression of SHARPIN. SHARPIN-expressing lentiviral vectors [pLV(Exp)-Puro-CMV>hSHARPIN(NM_030974.4)] and control vector [pLV(Exp)-Puro-CMV>ORF_Stuffer] were obtained from Vectorbuilder (https://en.vectorbuilder.com/). Lentiviral particles intended for infecting HCT116 cells were generated by transiently co-transfecting 293FT cells with the 2.5 μg of the specified plasmids and 1.8 μg of ViraPower Lentiviral Packaging Mix (Thermo Fisher Scientific, Inc.), following the manufacturer's protocol for Lipofectamine 3000 reagent (Thermo Fisher Scientific, Inc.). After a 48-h incubation at 37˚C, the viral supernatant was collected, and 1 ml was added to the HCT116 cells. The cells were transduced with lentiviral particles for 24 h, after which the medium was replaced. The cells were then subjected to selection using 2 μg/ml puromycin for 3 days, with 1 μg/ml puromycin used for maintenance. Subsequent experiments were then started. Non-cloned cells were utilized to maintain a heterogeneous cell population. Cells were validated as SHARPIN overexpressed clones using western blotting.

Murine xenograft model. All animal procedures were performed in compliance with the Guidelines for the Care and Use of Experimental Animals established by the Committee for Animal Experimentation of Kyusyu University (approval no. A22-364-0; Oita, Japan). All animal experiments were conducted following previously established protocols (25). A total of 12 female BALB/c nude mice (4-weeks-old; 16-19 g; Japan SLC, Inc.) were housed under specific pathogen-free conditions in the animal facility at the Kyushu University Beppu Hospital, with a 12/12-h light/dark cycle (light from 7:00 am to 7:00 pm) and controlled temperature maintained at 24±2˚C for optimal growth, while maintaining a relative humidity range of 50±10%. The mice were allowed *ad libitum* access to water and food pellets (CSF-1; Oriental Yeast Co., Ltd.). For subcutaneous xenograft assays, $1x10^6$ SHARPIN knockout RKO cells, HCT116 cells stably overexpressing SHARPIN, or control cells were suspended in 100 μl 50% Matrigel (Corning, Inc.) in PBS and bilaterally injected subcutaneously into nude mice. Mice were weighed, and tumor sizes were measured twice a week. Tumor volume was calculated using the formula: Length x $width^2$ x 0.5. At the end of the experiment, the mice were deeply anesthetized with 5% isoflurane for induction and 2% for maintenance (FUJIFILM Wako Pure Chemical Corporation) to minimize any potential pain or distress during the procedure, followed by cervical dislocation to sacrifice the mice.

Protein extraction and immunoblotting. To extract total protein, cells were lysed in lysis buffer (25 mM Tris-HCl at pH 7.5, 0.2 mM EDTA, 150 mM NaCl, 0.1% NP40, 5% glycerol) supplemented with proteinase inhibitor cocktail (BioVision, Inc.; Abcam) and PhosStop phosphatase inhibitor (Roche Diagnostics) on ice. Following sonication for 5 min, the lysates were centrifuged at 17,800 x g for 10 min at 4˚C. The resulting supernatants were collected, and protein concentrations were determined using the BCA Protein Assay Kit (Thermo Fisher Scientific, Inc.). Equal amounts of lysate were then boiled at 98˚C for 5 min with sodium dodecyl sulfate sample buffer. Immunoblotting analysis was conducted as previously described (35). In brief, equal quantities of protein (35 μg) were separated on 4-20% or 10% Tris-glycine polyacrylamide gels, followed by transfer to Immobilon-P Transfer Membranes (Merck Millipore) at 70 V for 4 h at room temperature or 30 V overnight at 4˚C. To block non-specific binding, membranes were incubated in blocking buffer (TBS and 0.1% Tween-20 with 5% nonfat milk powder) for 1 h at room temperature. Subsequently, the membranes were exposed to the following specific primary antibodies in blocking buffer overnight at 4˚C: SHARPIN (1:500; cat. no. 14626-1-AP; Proteintech Group, Inc.), MDM2 (1:1,000; cat. no. ab16895; Abcam), p53 (1:1,000; cat. no. ab1101; Abcam), p21 (1:200; cat. no. sc-6246; Santa Cruz Biotechnology, Inc.), BAX (1:1,000; cat. no. M010-3; MBL International Co.), PARP (1:1,000; cat. no. 9542; Cell Signaling Technology, Inc.) and β-actin (1:1,000; cat. no. sc-47778; Santa Cruz Biotechnology, Inc.). Following washing, the blots were exposed to the following secondary antibodies for 1 h at room temperature: Anti-rabbit (1:10,000; cat. no. NA934; Cytiva) and anti-mouse (1:10,000; cat. no. NA931; Cytiva). After another round of washing, detection was performed using the FUSION SOLO S (Vilber Lourmat). Band visualization was analyzed using ImageJ software (version 1.54 g; National Institutes of Health).

MTT assay. MTT assay were performed *in vitro* according to standard protocols, as previously described (24,25). In brief, cell proliferation was assessed using the Cell Proliferation Kit 1 (Roche Diagnostics) in accordance with the manufacturer's protocol. Cells were seeded at a density of 3,000 cells per well in triplicate onto 96-well plates with 100 μl of medium per

well. The purple formazan crystals formed were dissolved in isopropanol (FUJIFILM Wako Pure Chemical Corporation). The color reaction was measured using an iMark microplate reader (Bio-Rad Laboratories, Inc.) at 570 nm, with a reference filter set at 650 nm.

Colony formation assay. For knockout and overexpression experiments, cells were plated at a density of 2,000 cells/well in triplicates onto 6-well plates and incubated at 37˚C under 5% CO_2 with antibiotic selection. In the case of siRNA-mediated SHARPIN knockdown experiments, cells were plated overnight at the same density and incubated at 37˚C under 5% CO_2 overnight in antibiotic-free medium, followed by transfection with either siSHARPIN or negative control siRNA using Lipofectamine RNAiMAX (Thermo Fisher Scientific, Inc.) in triplicates. After a 14-day incubation period, colonies were stained using a Differential Quick Stain Kit (Sysmex Corporation) as per the manufacturer's protocol. Images of visible colonies were captured using a FUSION SOLO S (VILBER), and colonies containing >50 cells were counted and quantified using ImageJ software.

Apoptosis assay. RKO, LoVo and HCT116 cell lines were utilized for the apoptosis assay conducted *in vitro* following established protocols as previously described (25). Triplicate experiments were performed using the Annexin V-FITC Apoptosis Detection Kit (Abcam) according to the manufacturer's protocol. Subsequently, cells were analyzed using a SH800 cell sorter (Sony Biotechnology) and the results were analyzed using cell sorter software version 2.1.6 (Sony Biotechnology).

Cell cycle assay. Cells were synchronized in the G1 phase of the cell cycle via serum starvation for 72 h and re-stimulated by changing the medium containing 10% FBS. The cells were harvested, washed three times with PBS, and fixed in 70% ethanol at -20˚C overnight. The fixed cells were washed with PBS and incubated in 0.25 mg/ml RNase for 30 min at 37˚C. Subsequently, the cells were incubated in 5 mg/ml propidium iodide (Sigma Aldrich; Merck KGaA) for 30 min at room temperature in the dark. Cell cycle acquisition was performed on a SH800 cell sorter (Sony Biotechnology), and the results were analyzed using cell sorter software version 2.1.6 (Sony Biotechnology). The experiments were performed in triplicate to ensure statistical significance.

RNA sequencing (RNA-seq) analysis. RNA extracted from cells was sequenced using the DNBSEQ-G400 system at BGI. RNA samples were prepared using the Hieff NGS® Ultima Dual-mode RNA Library Prep Kit (cat. no.12309ES96; Shanghai Yeasen Biotechnology Co., Ltd.). The quality and integrity of the RNA samples were verified using an Agilent 2100 Bioanalyzer (cat. no. G2939BA; Agilent Technologies) and RNA 6000 Nano LabChip Kit (cat. no. 5067-1511; Agilent Technologies). The RNA Integrity Number was assessed to ensure high-quality samples suitable for sequencing. The sequencing was performed with a nucleotide length of 100 bp using paired-end sequencing (PE100). The sequencing kit used was the DNBSEQ-G400RS High-throughput Sequencing Set (FCL PE100) (cat. no. 1000016950; BGI). The final library concentration was measured in moles, specifically quantified using a Qubit fluorometer (Thermo Fisher Scientific, Inc.) and normalized to 10 pM for sequencing. The RNA-seq data were processed using SOAPnuke software for quality control and preprocessing, ensuring the removal of adaptor sequences, contamination and low-quality reads to obtain high-quality clean reads for downstream analysis. RNA-seq reads were obtained in fastq file format. The reads were aligned to the human reference sequence and gene annotations (UCSC hg19) using Tophat2 v2.1.1 (36). STAR v2.7.10b was used to calculate FPKM values (37). Differential expression analysis was conducted using DESeq2 (38).

Single-cell data processing. The 3' end scRNA-seq raw count matrix data (10X Genomics) of 370,115 cells and 43,113 genes from 64 patients with CRC was downloaded from GSE178341. The Python package Scanpy (v1.9.3) was used for processing in Python (https://scanpy.readthedocs.io/en/stable/). This downloaded dataset had already been processed by the author to remove low-quality cells and genes. The count matrix was normalized to 10,000 per cell by the total number of UMIs per cell and then log-transformed by adding one and standardized for each gene. Then, highly variable genes were selected using scanpy.pp.highly_variable_genes (n_top_genes=8000). Uniform manifold approximation and projection embeddings of the latent cell states of a single cell were conducted and visualized. The cell types already annotated by the author were used.

Spatial transcriptomics data processing. The raw count matrix data of the ST-seq dataset (10X Genomics) on 3313 spots was downloaded from one patient [named colon1 (ST-P1)] who did not receive neoadjuvant chemotherapy treatment. The Python package Scanpy (v1.9.3) was used for processing in Python. No spot filtering was performed for the subsequent integrated analysis. The count matrix was normalized and then log-transformed using scanpy.pp.normalize_total and scanpy.pp.log1p. Then, highly variable genes were selected using scanpy.pp.highly_variable_genes (n_top_genes=4000). Spatial feature expression plots were generated with scanpy.pl.spatial in Scanpy (v1.9.3).

Integration of spatial and scRNA-seq data. To augment cell-wise expression information into the spatial transcriptome and to perform cell-type deconvolution of spots in tissue sections, scRNA-seq was integrated with ST-seq using the deconvolution tool 'DeepCOLOR' (39). Raw count matrix data from scRNA-seq and ST-seq was used, which had 1,329 genes in common. The spatial distribution of all individual cells observed via scRNA-seq was determined by assessing the anticipated contribution of each individual cell to all spatial spots within the spatial transcriptome.

Enrichment analysis. Cluster-based detection of differentially expressed genes (DEGs) was performed using the Wilcoxon rank-sum test and Benjamini-Hochberg method to correct for multiple comparisons (scanpy.tl_rank_genes_groups). DEGs with an adjusted $P<0.05$ and log2 fold change >0 were included. Based on the DEGs, hallmark pathway analyses were performed using the Python package gseapy (v1.0.5).

Gene set enrichment analysis (GSEA). Associations between *SHARPIN* expression and previously defined gene sets were analyzed by GSEA using our RNA-seq data (40). Biologically defined gene sets were obtained from the Molecular Signatures Database v7.5 (http://software.broadinstitute.org/gsea/msigdb/index.jsp).

Statistical analysis. Variations among variables were compared using either the Mann-Whitney U test, unpaired Student's t-test, or Fisher's exact test where applicable. Multiple groups were analyzed by one-way ANOVA followed by Tukey's post hoc test. The Kaplan-Meier method was utilized to estimate overall survival (OS), and comparisons between survival curves were made using the log-rank test. Univariate and multivariate analyses were performed using Cox proportional hazards models to identify independent predictors of OS. The statistical analyses were performed using R software v4.2.0 and Python v3.9.16. $P<0.05$ was considered to indicate a statistically significant difference.

Results

SHARPIN is a potentially promotes tumor progression on Ch.8q in CRC. First, to identify a novel potential gene in CRC, bioinformatics analysis was conducted using the TCGA dataset. Frequent alterations in the copy numbers of specific chromosomal arms were observed, including 7p, 7q, 8q, 13p, 13q and 20q, in CRC (Fig. S1A). Additionally, as previously reported, this alteration occurs consistently in CRC development (22,23). Thus, it was aimed to identify novel potential genes located on Chromosome 8q. Focus was addressed on SHARPIN as a Ub-related gene in the TCGA dataset using the screening parameters outlined in the Material and Methods section (Fig. S1B). Next, RT-qPCR was conducted to assess *SHARPIN* mRNA expression levels in tumor and normal colon tissues from 111 patients with CRC. The analysis revealed significantly elevated *SHARPIN* mRNA expression in CRC tissues compared with normal colon tissues, consistent with findings from the TCGA dataset ($P<0.005$) (Fig. 1A). Furthermore, ~1/3 of the CRC cases in the TCGA dataset were p53 wild-type (Fig. S2A). Regardless of p53 status, *SHARPIN* mRNA was significantly elevated in tumor tissue compared with normal tissue (Fig. S2B). *SHARPIN* mRNA expression and copy number were positively correlated in the TCGA dataset ($R=0.71$, $P<0.01$) and CRC cell line dataset (Cancer Cell Line Encyclopedia) ($R=0.31$, $P<0.01$) (Fig. 1B). In addition, *SHARPIN* expression in CRC tissues was observed using public CRC scRNA-seq data (Fig. 1C). *SHARPIN* expression was higher in epithelial cells compared with other cells, with significantly higher expression in tumour epithelial cells than in normal epithelial cells (Fig. 1C and D). These results and the ST-seq dataset were further analysed in an integrated manner using DeepColor to confirm the distribution of epithelial cells only (Figs. 1E, F and S3). The data revealed that SHARPIN is specifically highly expressed in tumour epithelial cells and uniformly expressed in tumour cells (Fig. 1F). Immunohistochemical staining demonstrated that SHARPIN was localized in both the cytoplasm and nuclei of tumor cells, whereas SHARPIN staining was weak in normal epithelial cells (Fig. 1G). These observations suggested that SHARPIN is highly expressed in CRC cells. The frequency of mutations in SHARPIN was <1.0% in the COSMIC and TCGA databases (Fig. 1H). Taken together, these findings indicated that *SHARPIN* is overexpressed in CRC cells as a result of increased DNA copy numbers, and that amplification of SHARPIN on Chromosome 8q is a fundamental and prevalent occurrence in the tumorigenesis or progression of CRC.

Table II. Correlation between *SHARPIN* mRNA expression in tumor tissues and clinicopathological factors in our patients with colorectal cancer.

	Expression level of *SHARPIN* mRNA		
Variable	High (n=56)	Low (n=55)	P-value
Age, years (Mean ± SD)	67.3±9.47	67.1±10.9	0.91
Sex			
Male	34	32	0.85
Female	22	23	
Tumor size (cm)			
<3	9	11	0.63
≥3	47	44	
T stage			
1, 2	19	11	0.20
3, 4	36	44	
Lymphatic invasion			
-	26	38	<0.05
+	30	17	
Vascular invasion			
-	40	48	0.10
+	16	7	
Lymph node metastasis			
-	26	36	0.10
+	30	19	
Distant metastasis			
-	52	55	0.12
+	4	0	

SHARPIN, shank-associated RH domain interactor.

High expression of SHARPIN mRNA in tumor tissues predicts a poor prognosis in patients with CRC. The prognostic and clinical relevance of *SHARPIN* mRNA expression in CRC was evaluated. Initially, survival rates were assessed based on *SHARPIN* mRNA expression levels in patients with CRC. The OS rate was significantly lower in patients with high vs. low *SHARPIN* mRNA expression, both in TCGA and our CRC datasets (Fig. 1I). Furthermore, in the univariate analysis, a higher T stage, lymphatic invasion, vascular invasion, lymph node metastasis, distant metastasis and high *SHARPIN* mRNA expression were significantly associated with a lower

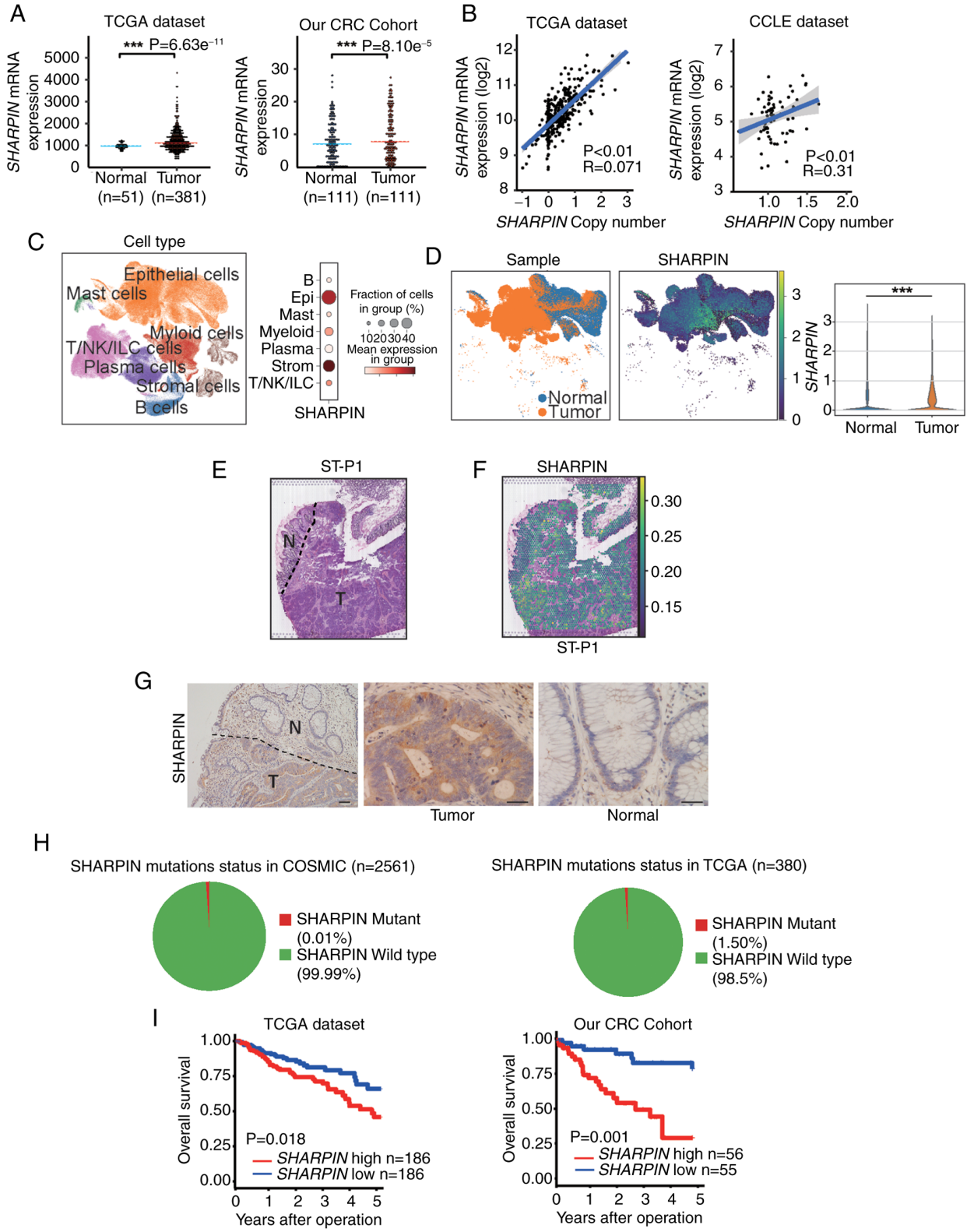

Figure 1. SHARPIN is a potential novel gene. (A) *SHARPIN* mRNA expression in CRC and normal colon tissues in TCGA and our CRC datasets. The dashed lines in the figure show the median of each group. (B) The correlation between DNA copy number and mRNA expression of *SHARPIN* in TCGA and CCLE datasets. R is the Pearson correlation coefficient. (C) SHARPIN expression in CRC tissues using public CRC single-cell RNA sequencing data. UMAP plot of the cell types in all cells (left). Dot plot of the expression proportions of SHARPIN per cell type (right). (D) UMAP plot of cell types after annotation of epithelial cells (left) and expression of *SHARPIN* in UMAP representation (middle). Violin plot of *SHARPIN* mRNA expression in normal vs. tumor tissues (right). (E) Pathological diagnosis distribution of a spatial transcriptomics slide. N, normal tissue; T, tumor tissue. (F) Spatial distribution of SHARPIN expression in epithelial cells in tissue sections analyzed using the deconvolution tool 'DeepCOLOR'. (G) Immunohistochemical staining of SHARPIN in CRC and normal tissues. N, normal tissue; T, tumor tissue. Scale bars, 200 μm (left) and 50 μm (middle and right). (H) Pie chart of SHARPIN mutation distribution in CRC cases of the COSMIC database (n=2,561) and TCGA (n=380). (I) Kaplan-Meier curves for the overall survival of patients with CRC according to *SHARPIN* mRNA expression in TCGA (n=372) and our CRC (n=111) datasets. The data are presented as the mean ± standard deviation. ***P<0.005. *SHARPIN*, shank-associated RH domain interactor; TCGA, The Cancer Genome Atlas; CRC, colorectal cancer; CCLE, Cancer Cell Line Encyclopedia; UMAP, Uniform Manifold Approximation and Projection; COSMIC, Catalogue of Somatic Mutations in Cancer.

OS rate. The multivariate Cox regression analysis revealed that high *SHARPIN* mRNA expression was an independent predictor of a poor prognosis in our CRC dataset (HR=3.29; 95% CI, 1.26-8.60, P<0.01) (Table I). These findings suggested that increased mRNA expression of *SHARPIN* is linked to a poorer prognosis in patients with CRC.

Clinicopathologic significance of SHARPIN mRNA expression in CRC tumor tissues. The relationship between SHARPIN mRNA expression and clinicopathological factors in patients with CRC treated at Kyushu University Beppu Hospital was examined (Table II). The patients were divided into two groups based on the median value of *SHARPIN* mRNA expression. A higher frequency of lymphatic invasion was found in the high (n=56) than low *SHARPIN* mRNA expression group (n=55). These findings indicated that elevated mRNA expression of *SHARPIN* associates positively with a malignant phenotype, particularly through lymphatic invasion.

SHARPIN is a potential therapeutic target for CRC. Inhibitors targeting E3 ubiquitin ligase (MDM2, BTRC, TRAF6, PRC1 and SKP2) have already been developed, and their antitumor effects have been reported (10-16). To investigate whether SHARPIN is a promising therapeutic target, a comprehensive analysis of 360 E3 ubiquitin ligase-related genes was performed and their potential efficacy as therapeutic targets was evaluated. It was determined whether high expression of the genes is associated with a poor prognosis and the correlation between mRNA expression and DNA copy number was calculated. Notably, SHARPIN was identified as the gene most strongly affected by copy number amplification, and its high mRNA expression and DNA copy number correlation in tumor tissues was associated with a poor prognosis, as shown in Fig. 2A. By contrast, *MDM2, BTRC, TRAF6, PRC1* and *SKP2,* which are currently being targeted by chemotherapeutic drugs (10,11,13-16), showed varying levels of upregulation in CRC tissues compared with normal tissues (Fig. 2B). Despite this upregulation, the correlation between their mRNA expression and copy number was less pronounced than that observed for SHARPIN, and these genes demonstrated no significant impact on the survival of patients with CRC in the TCGA dataset (Fig. 2C and D). These findings provide interesting evidence that SHARPIN may be the most promising therapeutic target among representative E3 ubiquitin ligase-related genes.

Pathway analysis of SHARPIN in CRC. To investigate the impact of SHARPIN on CRC, CRISPR/Cas9 technology was utilized to knock out SHARPIN in CRC cell lines (RKO and LoVo). Subsequently, RNA-seq analysis was performed on SHARPIN-knockout LoVo cells to explore the potential oncogenic pathways influenced by SHARPIN expression. This analysis revealed 533 significantly upregulated and 904 significantly downregulated genes in SHARPIN-knockout LoVo cells compared with non-target LoVo cells (Fig. 3A and B). Next, GSEA was performed to identify significant gene expression changes in SHARPIN-knockout cells and upregulation of numerous genes involved in apoptosis and p53-related pathways was observed (Fig. 3C). Furthermore, in tumor epithelial cells from scRNA-seq data, the cells were divided into high and low SHARPIN expression groups based on the median expression level of SHARPIN (Fig. 3D). Pathway analysis revealed that in the high expression group, pathways related to the cell cycle, apoptosis, and p53 were significantly enriched (Fig. 3E). These data suggested that SHARPIN expression is associated with the regulation of cell cycle, suppression of apoptosis and regulation of the p53 pathway in CRC cells.

SHARPIN promotes the proliferation of CRC cells in vitro. The impact of SHARPIN knockdown, knockout, or overexpression on the proliferation of CRC cell lines was investigated using MTT and colony formation assays. SHARPIN expression in p53 wild-type colon cancer cell lines, that is, RKO, LoVo and HCT116, was compared, with the more highly expressed RKO and LoVo cells used for knockdown and knockout experiments and the less highly expressed HCT116 for overexpression (Fig. S4A and B). SHARPIN was knocked out in CRC cell lines using the CRISPR/Cas9 system, and western blotting was conducted to confirm knockout (Fig. 4A). Furthermore, SHARPIN-knockout cells were transiently transfected with a vector encoding SHARPIN to restore its expression. Western blot analysis validated the successful rescue of SHARPIN expression in both SHARPIN-knockout RKO and LoVo cells (Fig. 4B). MTT assays revealed that the knockout of SHARPIN significantly inhibited cell proliferation in both RKO and LoVo cells (Fig. 4C). Colony formation assays showed that the knockout of SHARPIN significantly decreased colony formation in both RKO and LoVo cells (Fig. 4D). Similarly, SHARPIN knockdown by siRNA in RKO and LoVo cells revealed decreased proliferation (Fig. S4C and D). Next, HCT116 cells with stable overexpression of SHARPIN were established (Fig. 4E). As expected, SHARPIN overexpression significantly increased cell proliferation and colony formation (Fig. 4F and G). These results suggested that SHARPIN promotes proliferation of CRC cells *in vitro*.

SHARPIN promotes tumor growth in CRC in vivo. *In vivo* analyses were conducted using RKO cells with knockout of SHARPIN and HCT116 cells with stable overexpression of SHARPIN. SHARPIN knockout decreased the tumor volume (Fig. 5A). Immunohistochemical analysis of tumor xenografts indicated that tumor tissues derived from SHARPIN-knockout RKO cells exhibited reduced SHARPIN staining intensity and increased p53 staining intensity compared with non-target cells (Fig. 5B). Conversely, overexpression of SHARPIN increased the tumor volume in xenograft mouse models (Fig. 5C), and the tumor tissues from SHARPIN-overexpressing mice displayed stronger SHARPIN and weaker p53 staining compared with control tumor tissues (Fig. 5D). These results indicated that SHARPIN may promote tumor growth in CRC *in vivo* in response to changes in p53 expression.

SHARPIN suppresses apoptosis in CRC cells. Based on the pathway analysis (Fig. 3), it was hypothesized that SHARPIN promotes tumor growth by inhibiting apoptosis. To verify this hypothesis, western blot analysis was first performed. Compared with non-target cells, SHARPIN-knockout cells exhibited higher levels of cleaved poly (ADP-ribose)

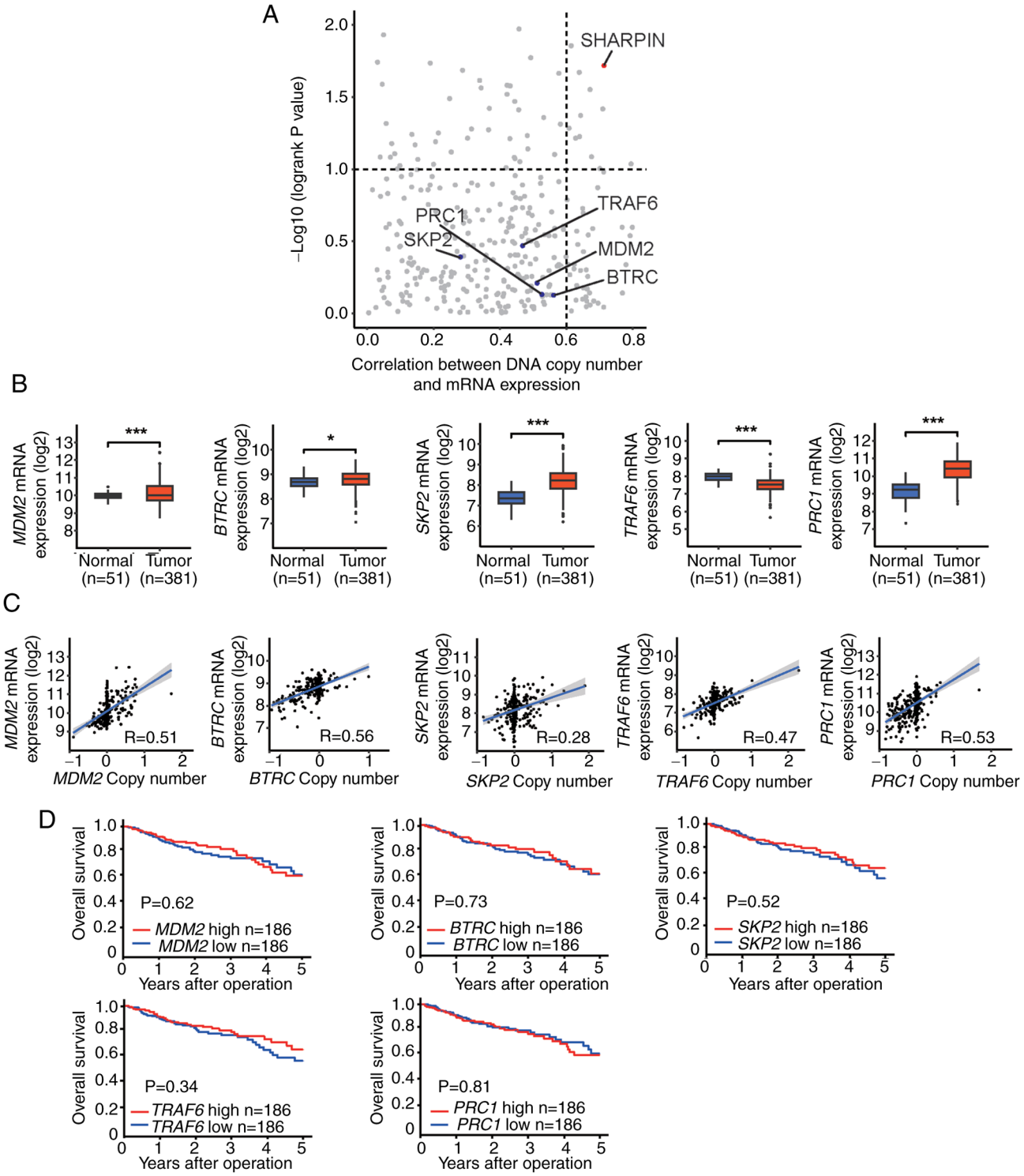

Figure 2. SHARPIN is a potential therapeutic target in CRC. (A) Statistical evaluation of 360 E3 ubiquitin ligase-related genes. Each gene is depicted as a dot on the graph, with its vertical position indicating the corrected P-value from the log-rank test (represented as-log10) and its horizontal position indicating the Pearson correlation coefficient between copy number and mRNA expression. The red dots represent SHARPIN and the blue dots MDM2, BTRC, SKP2, TRAF6 and PRC1. (B) mRNA expression of *MDM2*, *BTRC*, *SKP2*, *TRAF6* and *PRC1* in CRC and normal colon tissues in the TCGA dataset. (C) The correlation between the DNA copy number and mRNA expression of *MDM2*, *BTRC*, *SKP2*, *TRAF6* and *PRC1* in the TCGA dataset. (D) Kaplan-Meier curves for the OS of patients with CRC according to mRNA expression of *MDM2*, *BTRC*, *SKP2*, *TRAF6* and *PRC1* in the TCGA dataset (n=372). The data are presented as the mean ± standard deviation. *P<0.05 and ***P<0.005. *SHARPIN*, shank-associated RH domain interactor; CRC, colorectal cancer; TCGA, The Cancer Genome Atlas; OS, overall survival.

polymerase (PARP) and cleaved PARP/total PARP ratio, a molecular indicator of apoptosis (Fig. 6A). Moreover, knockout of SHARPIN resulted in an increased rate of apoptosis according to an apoptosis assay using fluorescence activated cell sorting (Fig. 6B). SHARPIN-overexpressing cells demonstrated a decreased level of a cleaved PARP and cleaved PARP/total PARP ratio (Fig. 6C), and a decreased rate of apoptosis (Fig. 6D). Furthermore, western blot analysis

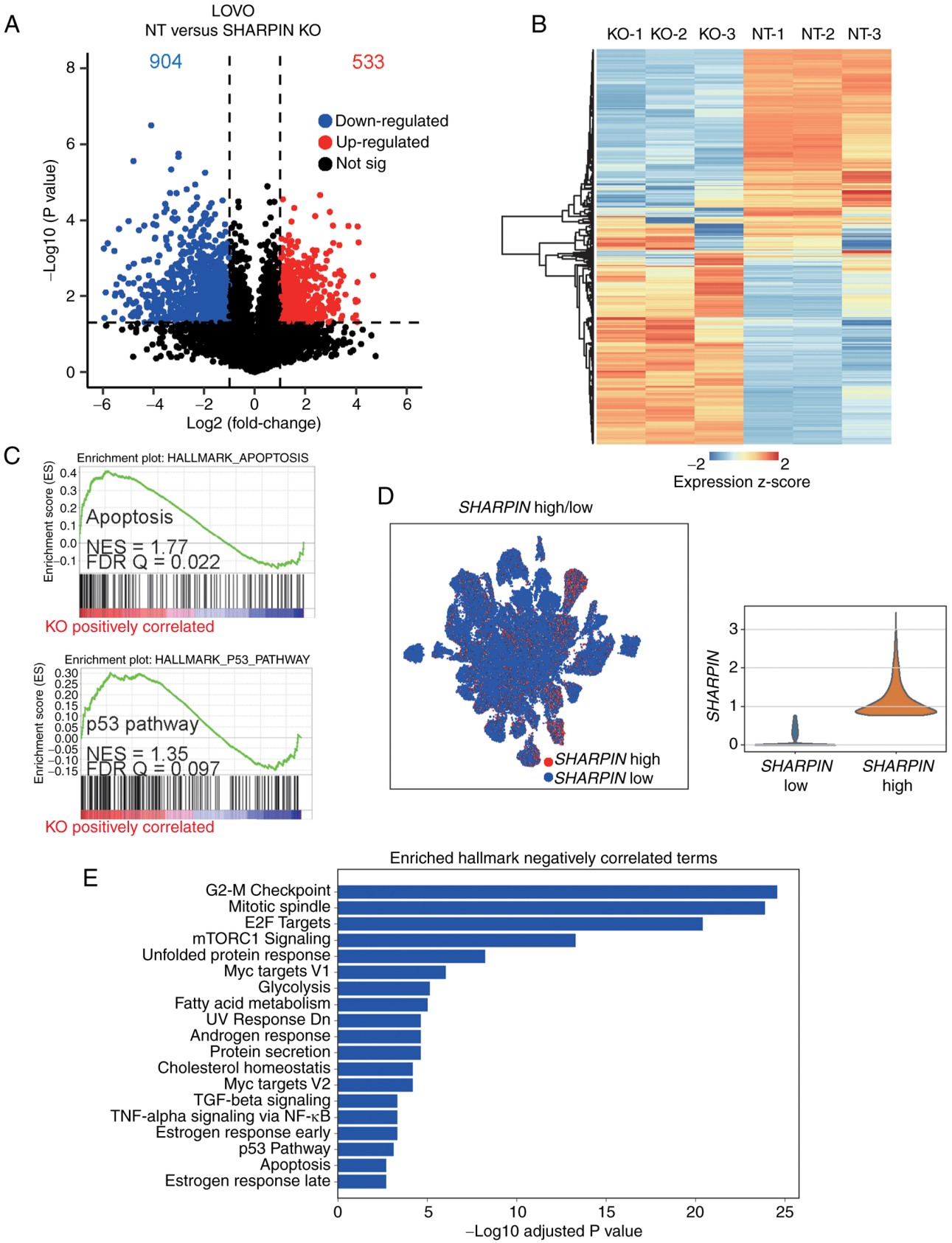

Figure 3. RNA sequencing of SHARPIN-knockout and non-target cells and enrichment pathway analysis of single-cell CRC data. (A) Volcano plot of the genes differentially expressed between non-target (NT) and SHARPIN-knockout (KO) LoVo cells. Upregulated genes are represented as red dots and downregulated genes as blue dots. (B) Heat map of mRNA expression changes between non-target and SHARPIN-knockout cells. (C) GSEA analysis of upregulated genes in SHARPIN knockout cells and GSEA plots of selected hallmark gene sets. (D) Tumor epithelial cells were extracted from scRNA-seq CRC data and divided into two groups by median expression of SHARPIN, with UMAP distribution showing carcinoma epithelial cells with high vs. low SHARPIN expression (left). Violin plots of cancer epithelial cells with high vs. low *SHARPIN* expression (right). (E) Hallmark pathway analysis of carcinoma epithelial cells with high vs. low *SHARPIN* expression. *SHARPIN*, shank-associated RH domain interactor; CRC, colorectal cancer; GSEA, Gene set enrichment analysis; FDR, false discovery rate; NES, normalized enrichment score; UMAP, Uniform Manifold Approximation and Projection.

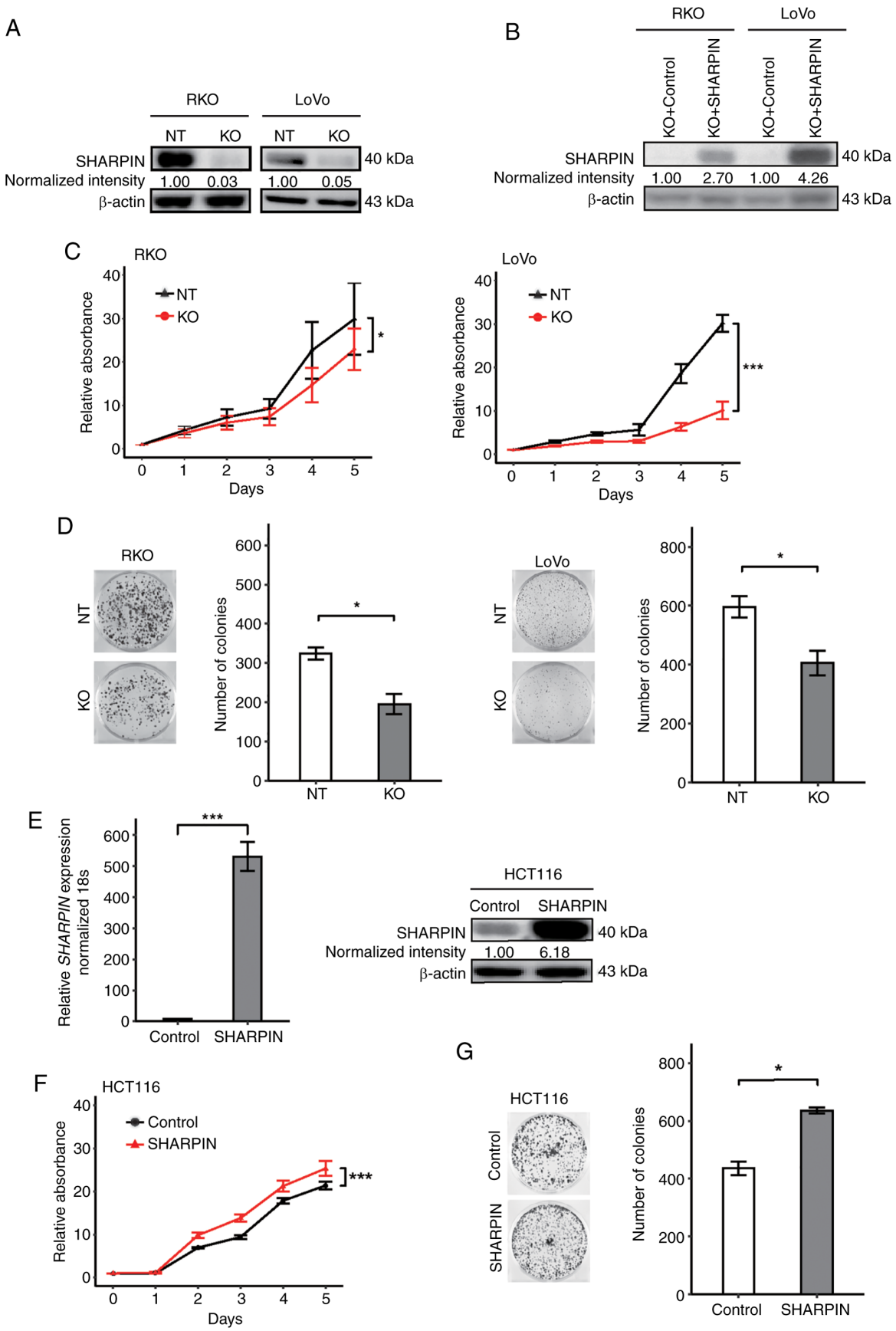

Figure 4. SHARPIN is associated with the growth of CRC *in vitro*. (A) Western blot analysis of SHARPIN in SHARPIN-KO and NT cells. (B) SHARPIN protein levels in the indicated cells. SHARPIN protein expression using western blot analysis in these rescued cells. (C) MTT assays in SHARPIN-knockout RKO and LoVo cells. (D) Colony formation assays in SHARPIN-knockout RKO and LoVo cells. (E) *SHARPIN* mRNA expression using reverse transcription□quantitative PCR and SHARPIN protein expression using western blot analysis in SHARPIN-overexpressing and control cells. (F) MTT assay in SHARPIN-overexpressing cells. (G) Colony formation assay in SHARPIN-overexpressing cells. The data are presented as the mean ± standard deviation. *P<0.05 and ***P<0.005. *SHARPIN*, shank-associated RH domain interactor; CRC, colorectal cancer; NT, non-target; KO, knockout.

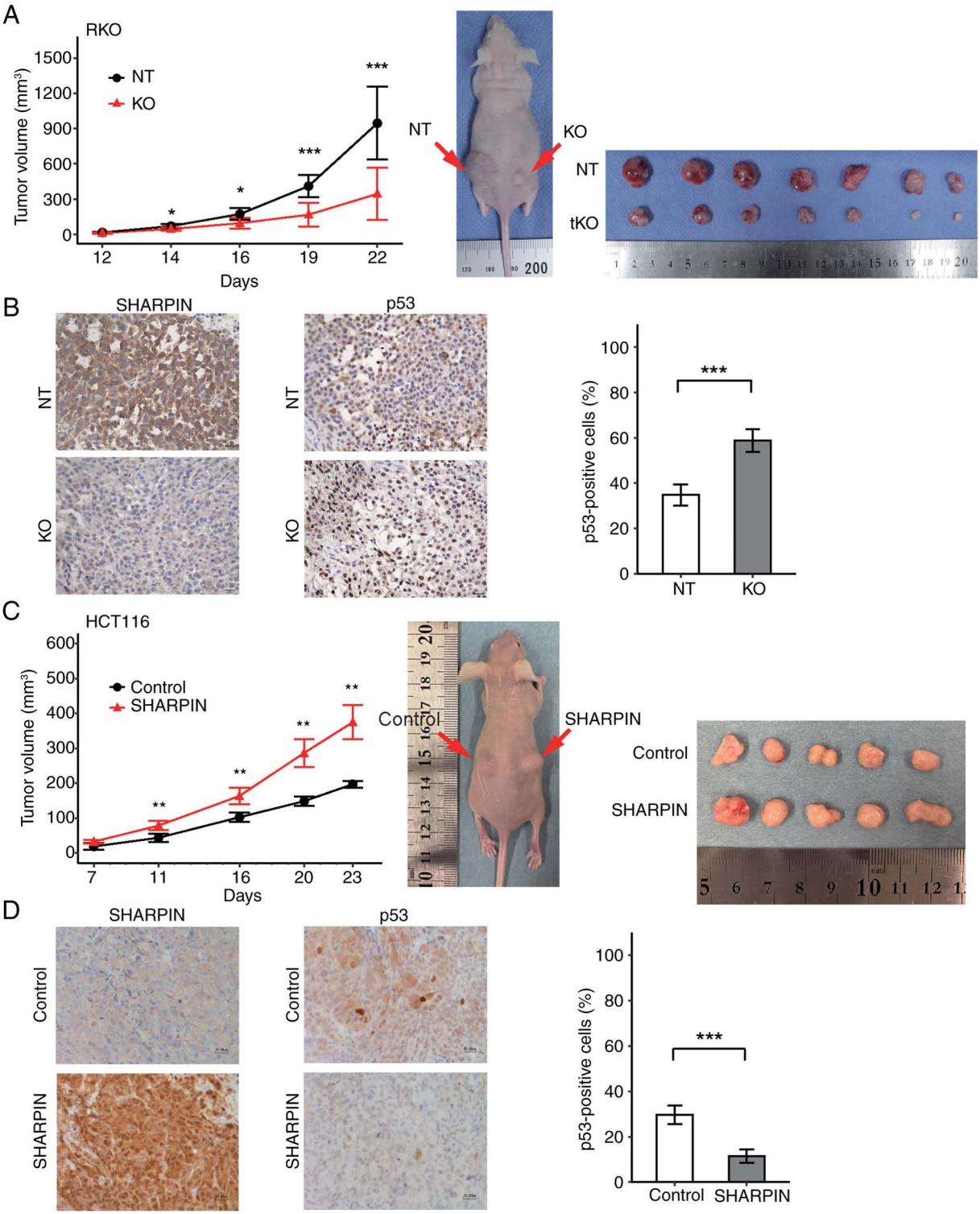

Figure 5. SHARPIN is associated with the growth of CRC *in vivo*. (A) *In vivo* analysis using a tumor xenograft model. Tumor size in xenograft models generated using NT or SHARPIN-KO CRC cells (n=7 per group). (B) Immunohistochemical staining of SHARPIN and p53 in tumor tissues from NT and KO CRC cells (left). Scale bars, 20 μm. The bar graphs represent the percentage of p53-positive cells in tumor tissues from KO (n=3) and NT (n=3) tumor tissues (right). (C) *In vivo* analysis using a tumor xenograft model. Tumor size in xenograft models generated using control cells and SHARPIN-overexpressing CRC cells (n=5) per group. (D) Immunohistochemical staining of SHARPIN and p53 in tumor tissues from control and SHARPIN-overexpressing CRC cells (left). Scale bars, 20 μm. The bar graphs represent the percentage of p53-positive cells in tumor tissues from SHARPIN-overexpressing (n=5) and control (n=5) tumor tissues (right). The data are presented as the mean ± standard deviation. *P<0.05, **P<0.01 and ***P<0.005. *SHARPIN*, shank-associated RH domain interactor; CRC, colorectal cancer; NT, non-target; KO, knockout.

was performed for p53-induced apoptotic genes, specifically BAX, in SHARPIN-knockout and SHARPIN-overexpressing cells and it was found that BAX expression increased in knockout cells and decreased in overexpressing cells (Fig. 6E). These findings indicated that SHARPIN slightly suppresses apoptosis in CRC cells.

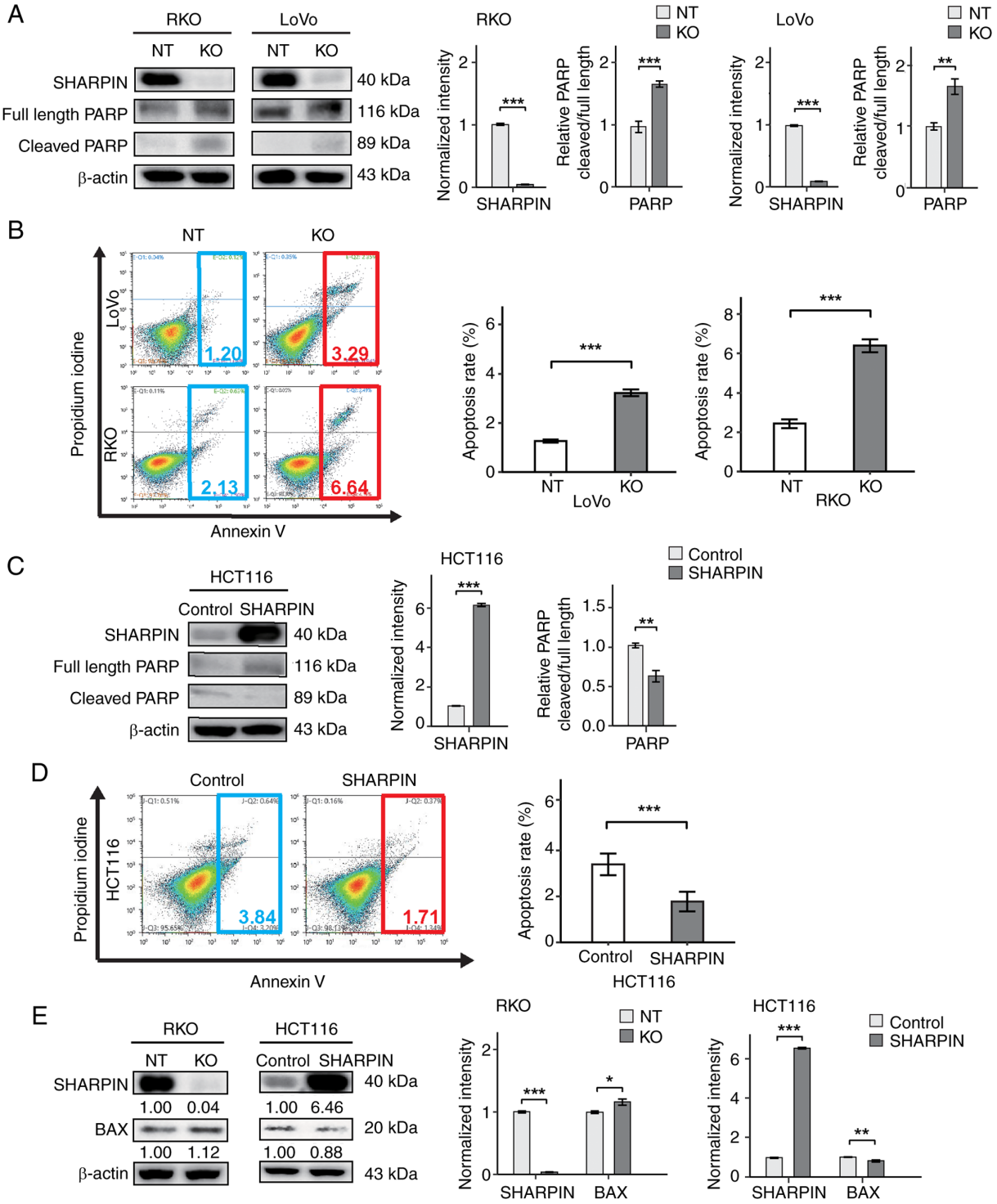

Figure 6. SHARPIN induces apoptosis in CRC cells. (A) Western blot analysis of SHARPIN, full-length PARP and cleaved PARP in SHARPIN-KO and NT cells. β-actin was used as the loading control. The right panel quantitatively displays the proteins from the left panel. (B) Left, Apoptosis assay of SHARPIN-KO LoVo (upper) and RKO (lower) cell lines. Right, Quantification of cell distribution in the apoptosis assay (Annexin V-FITC$^+$). (C) Western blot analysis of SHARPIN, full-length PARP and cleaved PARP in SHARPIN-overexpressing and control cells. β-actin was used as the loading control. The right panel quantitatively displays the proteins from the left panel. (D) Left, apoptosis assay of SHARPIN-overexpressing HCT116 cells. Right, quantification of cell distribution in the apoptosis assay. (E) Western blot analysis of SHARPIN and BAX in SHARPIN-KO, SHARPIN-overexpressing, and control cells. β-actin was used as the loading control. The right panel quantitatively displays the proteins from the left panel. The data are presented as the mean ± standard deviation. Statistical significance between groups was assessed using a two-tailed unpaired Student's t-test. *P<0.05, **P<0.01 and ***P<0.005. *SHARPIN*, shank-associated RH domain interactor; CRC, colorectal cancer; PARP, Poly (ADP-ribose) polymerase; NT, non-target; KO, knockout; BAX, Bcl-2-associated X protein.

SHARPIN promotes the cell cycle progression of CRC cells. Based on pathway analysis results derived from scRNA-seq data (Fig. 3E), it was hypothesized that SHARPIN may be involved in tumour growth by promoting cell cycle progression. Therefore, cell cycle analysis of SHARPIN knockout RKO cells was conducted using flow cytometry. It was observed

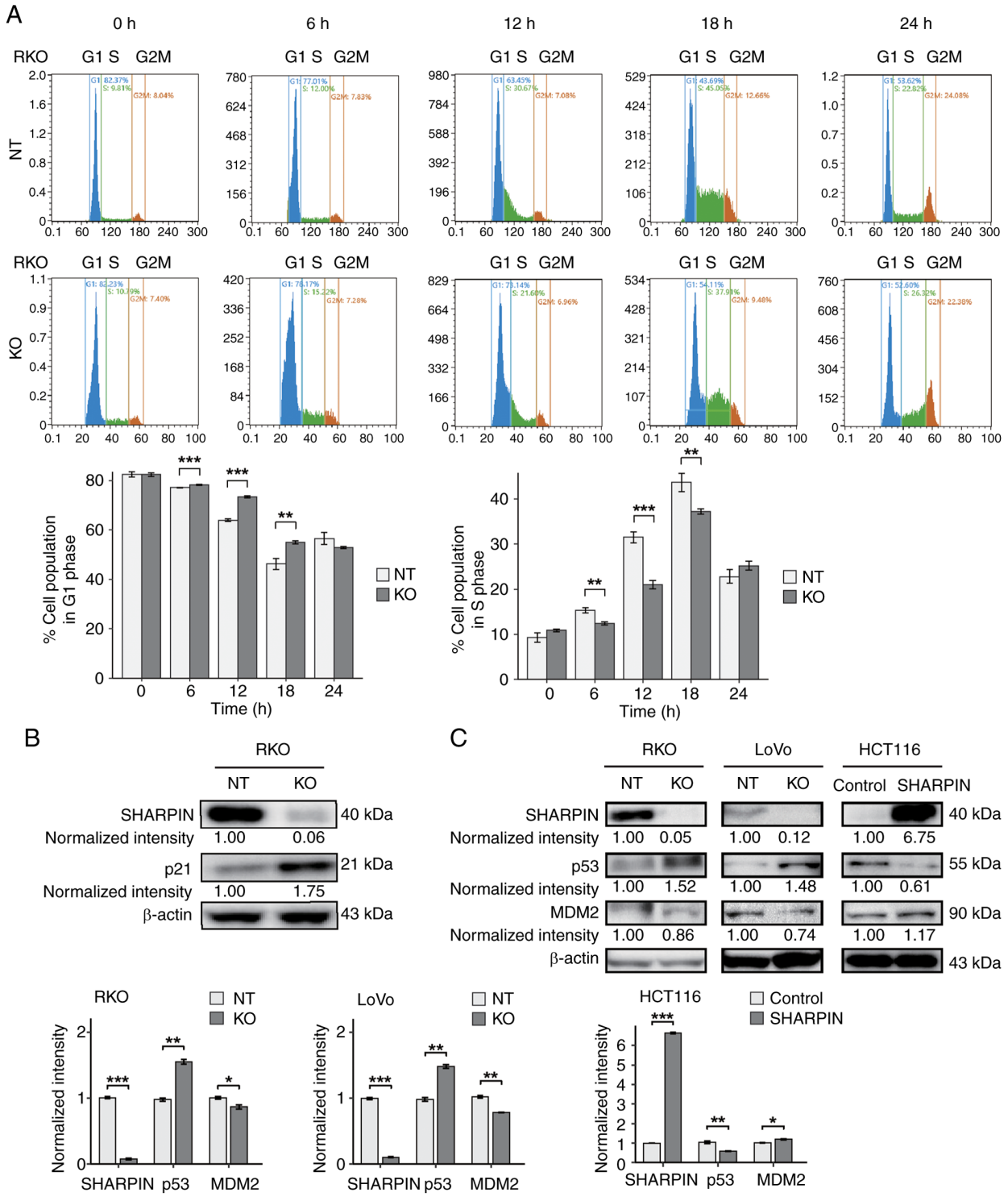

Figure 7. SHARPIN knockout prevents cell cycle progression via MDM2-dependent regulation of p53 expression in CRC cells. (A) Cell cycle assay of RKO control cells and SHARPIN-KO RKO cells. Propidium iodide staining was performed after refeeding of fetal bovine serum for the indicated time periods (upper). Bar graphs represent the percentage of cell distribution in G1 and S-phase (lower). (B) Western blot analysis of SHARPIN and p21 in control and SHARPIN-KO cells. β-actin was used as the loading control. (C) Western blot analysis of SHARPIN, MDM2 and p53 in SHARPIN-KO, SHARPIN-overexpressing and control cells. β-actin was used as the loading control. The lower panel quantitatively displays the proteins from the upper panel. Data are presented as the mean ± standard deviation. Statistical significance between groups was assessed using a two-tailed unpaired Student's t-test. *P<0.05, **P<0.01 and ***P<0.005. *SHARPIN*, shank-associated RH domain interactor; CRC, colorectal cancer; KO, knockout; NT, non-target.

that KO SHARPIN had a lower percentage of cells in S phase compared with NT at 6, 12 and 18 h after re-stimulation with medium containing 10% FBS (Fig. 7A). These results indicated that SHARPIN knockout inhibits the G1/S transition. To further investigate whether SHARPIN knockout inhibits the G1/S transition in CRC cells, western blot analysis showed that the expression of p21, which plays an important role in DNA damage repair at the G1/S cell cycle checkpoint, is increased (Fig. 7B). These results suggested that SHARPIN promotes the G1/S transition of the cell cycle in CRC cells.

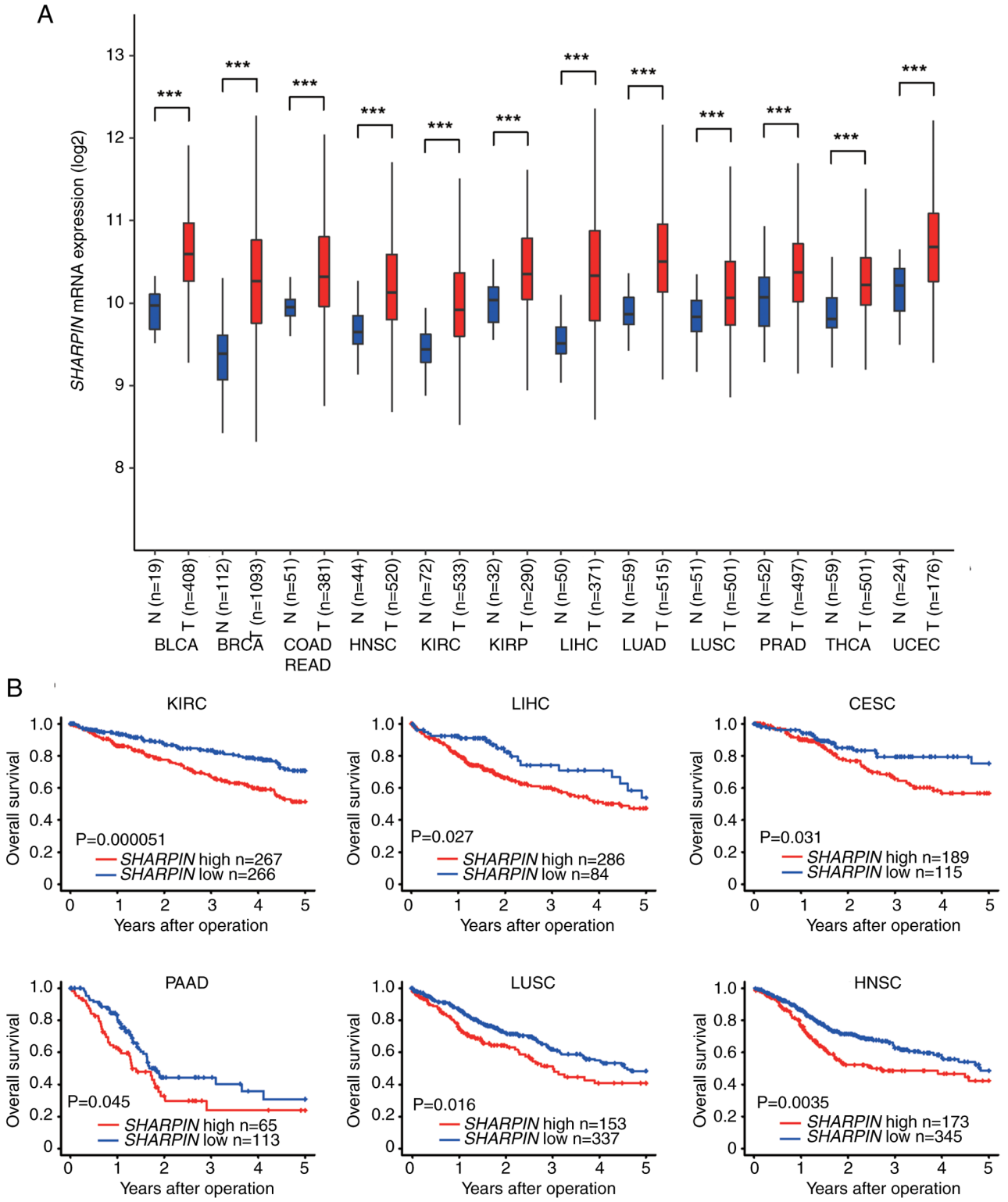

Figure 8. Pan-cancer analysis of *SHARPIN*. (A) mRNA expression of *SHARPIN* in various cancers. (B) Kaplan-Meier overall survival curves based on data from the indicated The Cancer Genome Atlas datasets. Data are presented as the mean ± standard deviation. ***P<0.005. *SHARPIN*, shank-associated RH domain interactor; BLCA, bladder urothelial carcinoma; BRCA, breast invasive carcinoma; CESC, cervical squamous cell carcinoma; COADREAD, colon adenocarcinoma and rectal adenocarcinoma; HNSC, head and neck squamous cell carcinoma; KIRC, kidney renal clear cell carcinoma; KIRP, kidney renal papillary cell carcinoma; LIHC, liver hepatocellular carcinoma; LUAD, lung adenocarcinoma; LUSC, lung squamous cell carcinoma; PAAD, pancreatic adenocarcinoma; PRAD, prostate adenocarcinoma; THCA, thyroid carcinoma; UCEC, uterine corpus endometrial carcinoma.

SHARPIN is involved in MDM2-dependent regulation of p53 expression. Pathway analysis using GSEA and single-cell analysis indicated that SHARPIN is associated with the p53 pathway (Fig. 3C and E). Western blot analysis was performed to verify the role of SHARPIN in the regulation of p53 expression. SHARPIN knockdown or knockout decreased MDM2 expression and increased p53 expression (Figs. 7C and S4E). On the other hand, SHARPIN overexpression increased

MDM2 expression and decreased p53 expression (Fig. 7C). These results are consistent with a previous study in breast cancer (41) reporting that SHARPIN increases MDM2 stability and promotes p53 degradation, suggesting that SHARPIN may be involved in MDM2-dependent regulation of p53 expression.

SHARPIN is overexpressed in various cancers. In the TCGA dataset, the expression of *SHARPIN* mRNA was compared between various cancer types and normal tissues. *SHARPIN* expression was found to be higher in 12 different cancer tissues, including CRC, compared with the expression levels in the respective non-cancerous tissues (Fig. 8A). Furthermore, high *SHARPIN* expression was associated with a poor prognosis in various cancer types (Fig. 8B). These findings suggested that SHARPIN may promote tumor growth in a variety of cancer types.

Discussion

SHARPIN is a constituent of the E3 ligase complex LUBAC, which activates NF-κB signaling, inflammation, embryogenesis and apoptosis by regulating the stability of targeted proteins such as PTEN, p53 and estrogen receptor alpha (41-45) via polyubiquitination or mono-ubiquitination. However, the clinical and biological significance of SHARPIN in CRC remains largely unknown. To the best of our knowledge, the present study represents the first attempt to investigate the role of SHARPIN, which could facilitate tumor growth and serve as a predictive biomarker of CRC.

Our clinical expression analysis including scRNA-seq and ST-seq identified that SHARPIN expression is significantly increased in CRC cells due to Ch.8p copy number amplification without somatic mutations. In addition, SHARPIN overexpression and its significant effect on survival have been observed in not only CRC but also various other types of cancers, as previously reported (41,45-47). These findings suggest that SHARPIN is a potential oncogene and a novel prognostic biomarker indicating poor outcomes for individuals with CRC.

In the present study, it was revealed that SHARPIN promotes tumor growth in CRC by promoting of cell cycle progression and suppressing apoptosis possibly mediated by decreasing p53 expression via increased MDM2 expression. The promotion of cell cycle progression by SHARPIN is likely due to decreased p21 expression mediated by p53, while the suppression of apoptosis is likely due to decreased BAX expression mediated by p53. Previous studies have demonstrated that SHARPIN facilitates p53 polyubiquitination and degradation in human breast cancer in an MDM2-dependent manner. In cholangiocarcinoma (45), inhibition of SHARPIN results in decreased p53 ubiquitination. Interestingly, NEDD4-1, an E3 ligase, is reported to ubiquitinate MDM2 with K63 type Ub chains followed by an increase in MDM2 protein stability by antagonizing the MDM2/MDMX complex, which ubiquitinates MDM2 with K48-linked degradative Ub chains in CRC cells (48). These findings suggested that SHARPIN may promote ubiquitination of MDM2, thereby enhancing MDM2 stability, leading to MDM2-dependent p53 degradation.

Previous clinical trials have demonstrated that E3 inhibitors targeting MDM2 and SKP2 are effective against various cancer types, including CRC (11,13). However, these drugs have significant side effects and limited efficacy compared with existing treatments. Of note, the present comprehensive analysis suggests that within CRC cells, SHARPIN demonstrates stable overexpression due to an increase in DNA copy number. Notably, SHARPIN exerts a more pronounced impact on the survival of patients with CRC compared with molecules undergoing clinical trials, such as MDM2 and SKP2. These findings indicated that SHARPIN has the potential to be a promising therapeutic target for CRC.

In the present study, it was discovered that SHARPIN promotes the progression of p53-wild type CRC. However, ~60% of actual CRC cases exhibit p53 mutations (49). Interestingly, SHARPIN has been reported to be involved in the progression of malignancies in a p53-independent manner. For example, SHARPIN modulates the NF-κB pathway in prostate cancer (46) or the p53/SLC7A11/GPX4 pathway in cholangiocarcinoma (45). Additionally, Versican expression cooperates synergistically with the Wnt/β-catenin pathway in hepatocellular carcinoma (47). These findings suggested that SHARPIN may facilitate CRC by regulating various malignant pathways. Further studies are needed to elucidate this mechanism.

In conclusion, the present study showed that SHARPIN functions in CRC, facilitating tumor growth through the promotion of cell cycle progression and inhibition of apoptosis, partly mediated by decreased p53 expression via increased MDM2 expression. Moreover, the expression of SHARPIN serves as a prognostic indicator for patients with CRC with poor outcomes. SHARPIN is a potential therapeutic target as well as prognostic biomarker in CRC.

Acknowledgements

The present study used the super-computing resource provided by the Human Genome Center, The Institute of Medical Science, The University of Tokyo (http://sc.hgc.jp/shiro kane.html). The authors would like to thank Ms. T. Fukuda, Ms. M. Kasagi, Ms. M. Sakuma, Ms. N. Mishima and Ms. T. Kawano from the Department of Surgery, Kyushu University Beppu Hospital (Oita, Japan) and Mr M. Utou from the Department of Clinical Laboratory Medicine, Kyushu University Beppu Hospital (Oita, Japan), for their technical assistance.

Funding

The present study was supported in part by the following grants and foundations: Japan Society for the Promotion of Science (JSPS) Grant-in-Aid for Science Research (grant nos. 19K09176, 19H03715, 20H05039, 20K08930, 20K17556, 21K07179, 22K02903, 22K09006, 23K06765 and 23K08074), the OITA Cancer Research Foundation (grant no. JP20cm0106475h0001), the AMED (grant nos. 23ck0106825h001, 23ck0106800h001, 22ama221501h0001, 21ck0106690s0201, 20ck0106547h0001 and 20ck0106541h0001), and the Takeda Science Foundation and The Princess Takamatsu Cancer Research Fund.

Availability of data and materials

The data generated in the present study may be found at the Gene Expression Omnibus under accession number

GSE255286 or at the following URL: (https://www.ncbi.nlm.nih.gov/geo/query/acc.cgi?acc=GSE255286). The data generated in the present study may be requested from the corresponding author.

Authors' contributions

YN conceived the study, conducted formal analysis and investigation, generated data visualizations, and wrote the original manuscript; contributing equally to data validation and methodological support. TM conceptualized the study and contributed equally to writing-reviewing and editing the manuscript, and supported supervision. TS, NT and TTob contributed to the collection of data and provided technical and material support. MH, TTa, HS, JT, KK, TA, YA, YO, KHi, KHo, SH and TI contributed to both data collection and analysis, and reviewed and edited the manuscript for important intellectual content. YH, TTos, YY, TO, MU, HE and YD contributed to the conception and design of the study, supervised the study and provided critical revisions to the manuscript. KM conceptualized and supervised the study, and contributed equally to writing-reviewing and editing the manuscript. YN and TM confirm the authenticity of all the raw data. All authors read and approved the final version of the manuscript.

Ethics approval and consent to participate

The present study was approved by the Kyushu University Institutional Review Board (approval no. 22244-00) and was performed in accordance with the tenets of the Declaration of Helsinki. Informed consent was obtained in the form of opt-out on the following website: https://www.beppu.kyushu-u.ac.jp/geka/information/clinical_disclosure/. Those who opted out were excluded. The animal experimental protocols were approved by the Animal Care and Use Committees of Kyushu University (approval no. A22-364-0; Oita, Japan), and all experiments were conducted in compliance with the institutional ethical guidelines for animal experiments and the safety guidelines for gene manipulation experiments.

Patient consent for publication

Not applicable.

Competing interests

The authors declare that they have no competing interests.

References

1. Varshavsky A: The ubiquitin system, an immense realm. Annu Rev Biochem 81: 167-176, 2012.
2. Dikic I: Proteasomal and autophagic degradation systems. Annu Rev Biochem 86: 193-224, 2017.
3. Welchman RL, Gordon C and Mayer RJ: Ubiquitin and ubiquitin-like proteins as multifunctional signals. Nat Rev Mol Cell Biol 6: 599-609, 2005.
4. Scheffner M, Nuber U and Huibregtse JM: Protein ubiquitination involving an E1-E2-E3 enzyme ubiquitin thioester cascade. Nature 373: 81-83, 1995.
5. Bence NF, Sampat RM and Kopito RR: Impairment of the ubiquitin-proteasome system by protein aggregation. Science 292: 1552-1555, 2001.
6. Bulatov E, Valiullina A, Sayarova R and Rizvanov A: Promising new therapeutic targets for regulation of inflammation and immunity: RING-type E3 ubiquitin ligases. Immunol Lett 202: 44-51, 2018.
7. Liu L, Zhang Y, Wong CC, Zhang J, Dong Y, Li X, Kang W, Chan FKL, Sung JJY and Yu J: RNF6 promotes colorectal cancer by activating the Wnt/β-catenin pathway via ubiquitination of TLE3. Cancer Res 78: 1958-1971, 2018.
8. Zhang Z, Chen J, Tang W, Feng Q, Xu J and Ren L: Comprehensive analysis reveals the potential regulatory mechanism between ub-proteasome system and cell cycle in colorectal cancer. Front Cell Dev Biol 14: 9:653528, 2021.
9. Shen J, Li P, Shao X, Yang Y, Liu X, Feng M, Yu Q, Hu R and Wang Z: The E3 ligase RING1 targets p53 for degradation and promotes cancer cell proliferation and survival. Cancer Res 78: 359-371, 2018.
10. Rasco DW, Lakhani NJ, Li Y, Men L, Wang H, Ji J, Tang Y, Liang Z, Amaya A, Estkowski K, *et al*: A phase I study of a novel MDM2 antagonist APG-115 in patients with advanced solid tumors. J Clin Oncol 37 (15 Suppl): S3126, 2019.
11. Stein EM, DeAngelo DJ, Chromik J, Chatterjee M, Bauer S, Lin CC, Suarez C, de Vos F, Steeghs N, Cassier PA, *et al*: Results from a first-in-human phase I study of siremadlin (HDM201) in patients with advanced wild-type TP53 solid tumors and acute leukemia. Clin Cancer Res 28: 870-881, 2022.
12. Masuda TA, Inoue H, Sonoda H, Mine S, Yoshikawa Y, Nakayama K, Nakayama K and Mori M: Clinical and biological significance of S-phase kinase-associated protein 2 (Skp2) gene expression in gastric carcinoma: Modulation of malignant phenotype by Skp2 overexpression, possibly via p27 proteolysis. Cancer Res 62: 3819-3825, 2002.
13. Dhillon N, Aggarwal BB, Newman RA, Wolff RA, Kunnumakkara AB, Abbruzzese JL, Ng CS, Badmaev V and Kurzrock R: Phase II trial of curcumin in patients with advanced pancreatic cancer. Clin Cancer Res 14: 4491-4499, 2008.
14. Nakajima H, Fujiwara H, Furuichi Y, Tanaka K and Shimbara N: A novel small-molecule inhibitor of NF-kappaB signaling. Biochem Biophys Res Commun 368: 1007-1013, 2008.
15. Brenke JK, Popowicz GM, Schorpp K, Rothenaigner I, Roesner M, Meininger I, Kalinski C, Ringelstetter L, R'kyek O, Jürjens G, *et al*: Targeting TRAF6 E3 ligase activity with a small-molecule inhibitor combats autoimmunity. J Biol Chem 293: 13191-13203, 2018.
16. Shukla S, Ying W, Gray F, Yao Y, Simes ML, Zhao Q, Miao H, Cho HJ, González-Alonso P, Winkler A, *et al*: Small-molecule inhibitors targeting Polycomb repressive complex 1 RING domain. Nat Chem Biol 17: 784-793, 2021.
17. Kirisako T, Kamei K, Murata S, Kato M, Fukumoto H, Kanie M, Sano S, Tokunaga F, Tanaka K and Iwai K: A ubiquitin ligase complex assembles linear polyubiquitin chains. EMBO J 25: 4877-4887, 2006.
18. Tokunaga F, Nakagawa T, Nakahara M, Saeki Y, Taniguchi M, Sakata S, Tanaka K, Nakano H and Iwai K: SHARPIN is a component of the NF-κB-activating linear ubiquitin chain assembly complex. Nature 471: 633-636, 2011.
19. Ikeda F, Deribe YL, Skånland SS, Stieglitz B, Grabbe C, Franz-Wachtel M, van Wijk SJ, Goswami P, Nagy V, Terzic J, *et al*: SHARPIN forms a linear ubiquitin ligase complex regulating NF-κB activity and apoptosis. Nature 471: 637-641, 2011.
20. Haas TL, Emmerich CH, Gerlach B, Schmukle AC, Cordier SM, Rieser E, Feltham R, Vince J, Warnken U, Wenger T, *et al*: Recruitment of the linear ubiquitin chain assembly complex stabilizes the TNF-R1 signaling complex and is required for TNF-mediated gene induction. Mol Cell 36: 831-844, 2009.
21. Davoli T, Xu AW, Mengwasser KE, Sack LM, Yoon JC, Park PJ and Elledge SJ: Cumulative haploinsufficiency and triplosensitivity drive aneuploidy patterns and shape the cancer genome. Cell 155: 948-962, 2013.
22. Saito T, Niida A, Uchi R, Hirata H, Komatsu H, Sakimura S, Hayashi S, Nambara S, Kuroda Y, Ito S, *et al*: A temporal shift of the evolutionary principle shaping intratumor heterogeneity in colorectal cancer. Nat Commun 9: 2884, 2018.
23. Uchi R, Takahashi Y, Niida A, Shimamura T, Hirata H, Sugimachi K, Sawada G, Iwaya T, Kurashige J, Shinden Y, *et al*: Integrated multiregional analysis proposing a new model of colorectal cancer evolution. PLoS Genet 12: e1005778, 2016.
24. Kouyama Y, Masuda T, Fujii A, Ogawa Y, Sato K, Tobo T, Wakiyama H, Yoshikawa Y, Noda M, Tsuruda Y, *et al*: Oncogenic splicing abnormalities induced by DEAD-Box Helicase 56 amplification in colorectal cancer. Cancer Sci 110: 3132-3144, 2019.

25. Sato K, Masuda T, Hu Q, Tobo T, Gillaspie S, Niida A, Thornton M, Kuroda Y, Eguchi H, Nakagawa T, *et al*: Novel oncogene 5MP1 reprograms c-Myc translation initiation to drive malignant phenotypes in colorectal cancer. EBioMedicine 44: 387-402, 2019.
26. Kobayashi Y, Masuda T, Fujii A, Shimizu D, Sato K, Kitagawa A, Tobo T, Ozato Y, Saito H, Kuramitsu S, *et al*: Mitotic checkpoint regulator RAE1 promotes tumor growth in colorectal cancer. Cancer Sci 112: 3173-3189, 2021.
27. Sampson C, Wang Q, Otkur W, Zhao H, Lu Y, Liu X and Piao HL: The roles of E3 ubiquitin ligases in cancer progression and targeted therapy. Clin Transl Med 13: e1204, 2023.
28. Hashiguchi Y, Muro K, Saito Y, Ito Y, Ajioka Y, Hamaguchi T, Hasegawa K, Hotta K, Ishida H, Ishiguro M, *et al*: Japanese society for cancer of the colon and rectum (JSCCR) guidelines 2019 for the treatment of colorectal cancer. Int J Clin Oncol 25: 1-42, 2020.
29. Masuda TA, Inoue H, Nishida K, Sonoda H, Yoshikawa Y, Kakeji Y, Utsunomiya T and Mori M: Cyclin-dependent kinase 1 gene expression is associated with poor prognosis in gastric carcinoma. Clin Cancer Res 9: 5693-5698, 2003.
30. Wittwer CT, Ririe KM, Andrew RV, David DA, Gundry RA and Balis UJ: The LightCycler: A microvolume multisample fluorimeter with rapid temperature control. Biotechniques 22: 176-181, 1997.
31. Yguerabide J and Ceballos A: Quantitative fluorescence method for continuous measurement of DNA hybridization kinetics using a fluorescent intercalator. Anal Biochem 228: 208-220, 1995.
32. Ueda M, Iguchi T, Nambara S, Saito T, Komatsu H, Sakimura S, Hirata H, Uchi R, Takano Y, Shinden Y, *et al*: Overexpression of transcription termination factor 1 is associated with a poor prognosis in patients with colorectal cancer. Ann Surg Oncol 22 (Suppl 3): S1490-S1498, 2015.
33. Sanjana NE, Shalem O and Zhang F: Improved vectors and genome-wide libraries for CRISPR screening. Nat Methods 11: 783-784, 2014.
34. Shalem O, Sanjana NE, Hartenian E, Shi X, Scott DA, Mikkelson T, Heckl D, Ebert BL, Root DE, Doench JG and Zhang F: Genome-scale CRISPR-Cas9 knockout screening in human cells. Science 343: 84-87, 2014.
35. Hirata H, Sugimachi K, Komatsu H, Ueda M, Masuda T, Uchi R, Sakimura S, Nambara S, Saito T, Shinden Y, *et al*: Decreased expression of fructose-1,6-bisphosphatase associates with glucose metabolism and tumor progression in hepatocellular carcinoma. Cancer Res 76: 3265-3276, 2016.
36. Trapnell C, Roberts A, Goff L, Pertea G, Kim D, Kelley DR, Pimentel H, Salzberg SL, Rinn JL and Pachter L: Differential gene and transcript expression analysis of RNA-seq experiments with TopHat and Cufflinks. Nat Protoc 7: 562-578, 2012.
37. Dobin A, Davis CA, Schlesinger F, Drenkow J, Zaleski C, Jha S, Batut P, Chaisson M and Gingeras TR: STAR: ultrafast universal RNA-seq aligner. Bioinformatics 29: 15-21, 2013.
38. Love MI, Huber W and Anders S: Moderated estimation of fold change and dispersion for RNA-seq data with DESeq2. Genome Biol 15: 550, 2014.
39. Kojima Y, Mii S, Hayashi S, Hirose H, Ishikawa M, Akiyama M, Enomoto A and Shimamura T: Single-cell colocalization analysis using a deep generative model. bioRxiv: 2022.2004.2010.487815, 2022.
40. Subramanian A, Tamayo P, Mootha VK, Mukherjee S, Ebert BL, Gillette MA, Paulovich A, Pomeroy SL, Golub TR, Lander ES and Mesirov JP: Gene set enrichment analysis: A knowledge-based approach for interpreting genome-wide expression profiles. Proc Natl Acad Sci USA 102: 15545-15550, 2005.
41. Yang H, Yu S, Wang W, Li X, Hou Y, Liu Z, Shi Y, Mu K, Niu G, Xu J, *et al*: SHARPIN facilitates p53 degradation in breast cancer cells. Neoplasia 19: 84-92, 2017.
42. De Melo J, Lin X, He L, Wei F, Major P and Tang D: SIPL1-facilitated PTEN ubiquitination contributes to its association with PTEN. Cell Signal 26: 2749-2756, 2014.
43. Zhuang T, Yu S, Zhang L, Yang H, Li X, Hou Y, Liu Z, Shi Y, Wang W, Yu N, *et al*: SHARPIN stabilizes estrogen receptor α and promotes breast cancer cell proliferation. Oncotarget 8: 77137-77151, 2017.
44. Zeng C, Xiong D, Zhang K and Yao J: Shank-associated RH domain interactor signaling in tumorigenesis. Oncol Lett 20: 2579-2586, 2020.
45. Zeng C, Lin J, Zhang K, Ou H, Shen K, Liu Q, Wei Z, Dong X, Zeng X, Zeng L, *et al*: SHARPIN promotes cell proliferation of cholangiocarcinoma and inhibits ferroptosis via p53/SLC7A11/GPX4 signaling. Cancer Sci 113: 3766-3775, 2022.
46. Zhang Y, Huang H, Zhou H, Du T, Zeng L, Cao Y, Chen J, Lai Y, Li J, Wang G and Guo Z: Activation of nuclear factor κB pathway and downstream targets survivin and livin by SHARPIN contributes to the progression and metastasis of prostate cancer. Cancer 120: 3208-3218, 2014.
47. Tanaka Y, Tateishi K, Nakatsuka T, Kudo Y, Takahashi R, Miyabayashi K, Yamamoto K, Asaoka Y, Ijichi H, Tateishi R, *et al*: Sharpin promotes hepatocellular carcinoma progression via transactivation of Versican expression. Oncogenesis 5: e277, 2016.
48. Xu C, Fan CD and Wang X: Regulation of Mdm2 protein stability and the p53 response by NEDD4-1 E3 ligase. Oncogene 34: 281-289, 2015.
49. Kandoth C, McLellan MD, Vandin F, Ye K, Niu B, Lu C, Xie M, Zhang Q, McMichael JF, Wyczalkowski MA, *et al*: Mutational landscape and significance across 12 major cancer types. Nature 502: 333-339, 2013.

Copyright © 2024 Nakano et al. This work is licensed under a Creative Commons Attribution-NonCommercial-NoDerivatives 4.0 International (CC BY-NC-ND 4.0) License.